

A. Operational transconductance amplifier - OTA

The topology of OTA is shown in the Fig. 3. This circuit is based on parallel connection of two-stage NMOS and PMOS OPAMPs working in sub-threshold regimes.

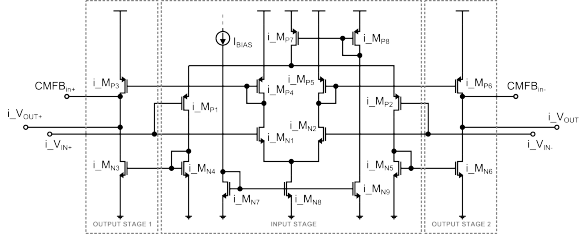


Fig. 3. Topology of OTA

Complementary connection of NMOS and PMOS in the OPAMP output stage allows R_tR operation at output. It is well-known that input voltage range of PMOS transistor is limited from above by the voltage:

$$V_{PMOS_{MAX}} = V_{DD} - |V_{DS_{sat}}(i_{MP7})| - |V_{TH}(i_{MP1})| \quad (1)$$

In the range from $V_{PMOS_{MAX}}$ to V_{DD} is NMOS transistor active only. Contrariwise, the input voltage range of NMOS transistor is limited from below by the voltage:

$$V_{NMOS_{MIN}} = V_{DS_{sat}}(i_{MN8}) + V_{TH}(i_{MN1}) \quad (2)$$

In the range from ground to $V_{NMOS_{MIN}}$ is PMOS transistor active only.

Around the $\frac{V_{DD}}{2}$ voltage, both of transistors are in the active region. In the area where both amplifiers operate in the active region, the transconductances $g_{m_{NMOS}}$ and $g_{m_{PMOS}}$ are overlapped. In general, by increasing g_m , the dominant pole is shifted towards higher frequencies. This may result in frequency response and overall circuit stability. Transistors i_{MN1} , i_{MN2} , i_{MP1} and i_{MP2} have been designed with g_m compensation as is shown in Fig. 4:

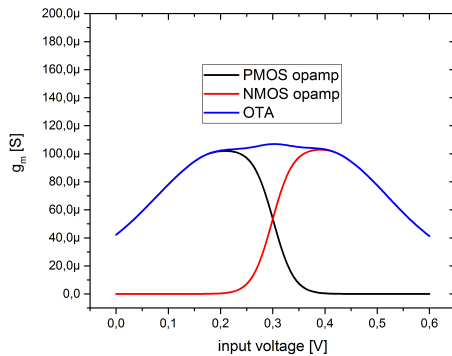


Fig. 4. Compensation of $g_{m_{PMOS}}$ and $g_{m_{NMOS}}$

The input transistors (i_{MN1} , i_{MN2} , i_{MP1} , i_{MP2}) was set to the sub-threshold region by the equations:

$$V_{eff} = 2 \cdot V_T \cdot n \cdot \ln(\exp(\sqrt{IF}) - 1) \quad (3)$$

$$\frac{W}{L} = \frac{I_D}{I_{D0} \cdot \exp\left(\frac{V_{eff}}{n \cdot V_T}\right)} \quad (4)$$

The current sources (i_{MP7} , i_{MN8}) works in strong saturation by the V_{DS} voltage approximately 100 mV. Transistors i_{MN7} , i_{MN9} and i_{MP8} was used as the simple current mirrors for circuit biasing. i_{MP4} , i_{MP5} , i_{MN4} and i_{MN5} was used as a current mirrors for output stage 1 and 2 [5].

As an output stage, AB class amplifier is used. Dimensions of the transistors i_{MP3} , i_{MN3} , i_{MP6} and i_{MN6} was designed for relatively high currents in that branches due to driving output capacitors and capacitors in CMFB circuit.

B. Clock-boost circuit

In order to control switching transistors in CMFB circuit clock-boost circuit was used. Its topology is shown in the Fig. 5. Two inverters at the beginning of the circuit modify the rising and the falling edges of the clock signal for better operate with. Cross-coupled NMOS transistors b_{MN1} and b_{MN2} together with the capacitors b_{C1} and b_{C2} are forming a charge pump. Pulses from the clock are shifted up by adding V_{DD} voltage to them. By the transistors b_{MN3} and b_{MN4} is this shifted voltage (in the other words: shifted charge) connected to a "bootstrap" capacitor b_{C3} . By switching the transistors b_{MP1} , b_{MN5} , b_{MP2} , b_{MN6} , b_{MN7} , b_{MN8} and b_{MN9} is mentioned charge transported to the output - switching transistor in SC CMFB circuit. This circuit was designed as a part of SC CMFB circuit as a "bootstrap" [2].

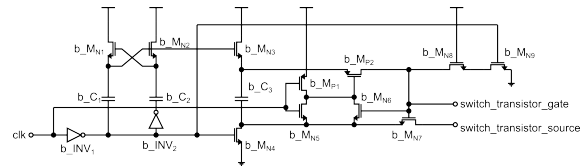


Fig. 5. Topology of clock-boost circuit

C. Switched-capacitor CMFB circuit

Fig. 6 shows the topology of the SC CMFB circuit. There are three task for CMFB circuit: sensing the common mode outputs i_{VOUT+} and i_{VOUT-} from fully differential OTA, comparison of the sensed results with a reference voltage V_{CM} (in this design, the reference voltage for CMFB circuit is equal to $\frac{V_{DD}}{2}$) and return the bias voltage V_{BIAS} back to the OTA by $CMFB$ output. This SC CMFB circuit is clocked by non-overlapping pulses with frequency $f_{sw} = 20 \text{ MHz}$. These pulses are shifted up in "bootstrap" circuits for better gate-switching of all the

transistors in the Fig. 6 [2]. All the transistors have been designed with the same dimensions as a switches with a low enough R_{ON} parameter. The capacitors cm_C_1 (cm_C_2) and cm_C_3 (cm_C_4) have been designed with a specific ratio k :

$$k = \frac{cm_C_1}{cm_C_3} = \frac{cm_C_2}{cm_C_4} \quad (5)$$

In order to obtain low value of output offset, the specific ratio capacitors cm_C_1 (cm_C_2) and cm_C_3 (cm_C_4) should be perfectly set. However, cm_C_1 and cm_C_2 can not be too large, because OTA will not be able to drive them. On the contrary, cm_C_3 and cm_C_4 can not be too small, because the parasitic capacitance of the switching transistors will start to affect the circuit. Transistors cm_M_{P1} , cm_M_{P2} , cm_M_{N9} and cm_M_{N10} form the output invertors for driving the SC CMFB outputs. These outputs are connected to the OTA, as it is shown in the Fig. 2 and Fig. 3.

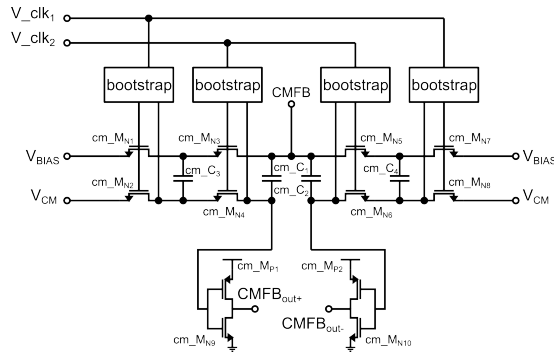


Fig. 6. Topology of switched-capacitor CMFB circuit

D. Switching transmission gates (T-gates)

As it is shown in the Fig 2., capacitors i_C_{S1} - i_C_{S4} are switched with transmission gates (T-gates) i_T_1 - i_T_8 for better charge transport. For initial values of capacitors, voltage gain and cutoff frequency the following equations can be used:

$$C_{sw} \propto \frac{1}{f_{sw} \cdot R_{eq}} \quad (6)$$

$$A_{INT_MAX} \propto \frac{i_C_{S1}}{i_C_{S3}} \quad (7)$$

$$f_{cutoff} = BW_{INT} \propto \frac{1}{2 \cdot \pi \cdot i_C_1 \cdot R_{eq}(i_C_{S3})} \quad (8)$$

III. ACHIEVED RESULTS

The integrator has been simulated with the signals of varying frequencies, amplitudes and types. For DC simulation of the OTA (with disconnected SC CMFB circuit), the input voltage was swept in the range of GND and V_{DD} . In the AC simulation, two periodic sources with 180° phase shift were used for simulate differential input signal. Because of using clocks, periodic steady-state analysis (PSS analysis) and periodic AC analysis (PAC analysis) was

used. In the Fig. 7 are shown the transfer responses of inverting and non-inverting outputs, where R_{iR} output voltage range can be obtained. Fig. 8 shows frequency response of OTA with maximum gain of $A_{OTA_MAX} = 46.16$ dB. Bandwidth of proposed OTA is $BW_{OTA} = 24.23$ kHz, while gain-bandwidth is $GBW = 5.03$ MHz.

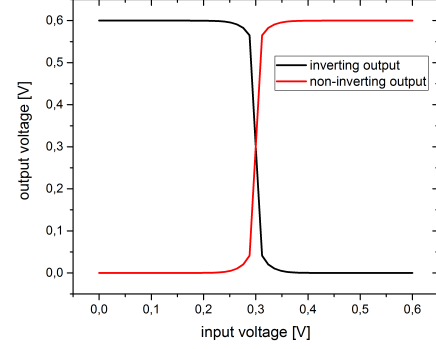


Fig. 7. Transfer response of OTA

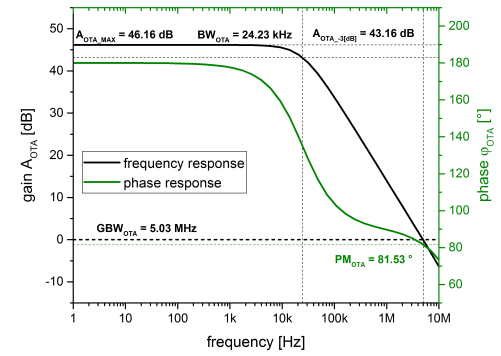


Fig. 8. Frequency and phase response of OTA

Fig. 9 shows frequency response of whole integrator where low-frequency gain of $A_{INT_MAX} = 24.09$ dB and cutoff frequency $f_{cutoff} = 165.95$ kHz were achieved.

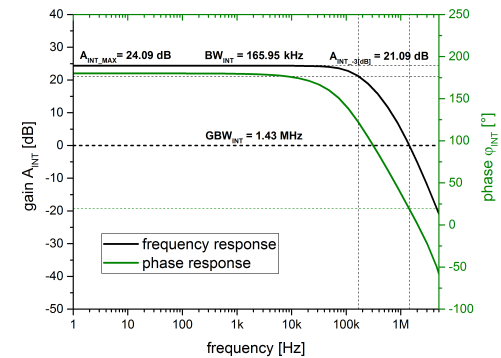


Fig. 9. Frequency and phase response of integrator

In Fig. 10 is shown time response of integrator to a harmonic input signal and Fig. 11 shows time response of integrator to a pulse input signal.

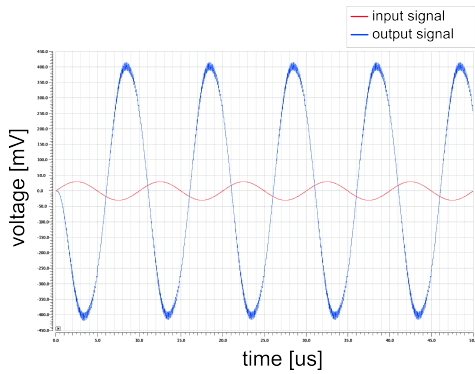


Fig. 10. Harmonic signal response - integration

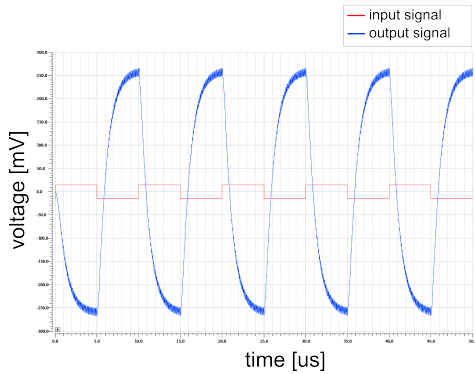


Fig. 11. Pulse signal response - integration

All the essential achieved parameters are summarized in the Tab. 1.

TABLE I. INTEGRATOR PARAMETERS

Parameter	Value
V_{DD}	0.6 V
C_{LOAD}	10 pF
A_{OTA_MAX}	46.16 dB
BW_{OTA}	24.23 kHz
GBW_{OTA}	5.03 MHz
PM_{OTA}	81.53°
A_{INT_MAX}	24.09 dB
BW_{INT}	165.95 kHz
GBW_{INT}	1.43 MHz
P_{INT}	22.16 μW

In addition, interesting thing is the effect of the dimensions of transistor to shape of the switched signal. In the Fig. 12 is the signal switched by NMOS transistor of small dimensions.

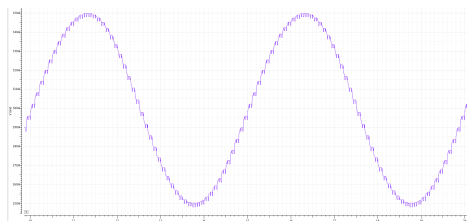


Fig. 12. Switched signal - W and L small enough

In the Fig. 13 is this signal switched by NMOS transistor with the same width as in the Fig. 12, but with increased length.

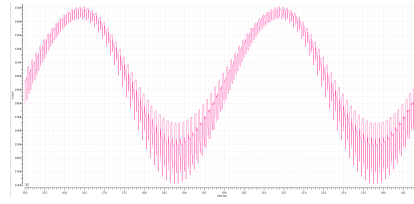


Fig. 13. Switched signal - small W, larger L

In the Fig. 14 is this signal switched by NMOS transistor with the same length as in the Fig. 12, but with increased width.

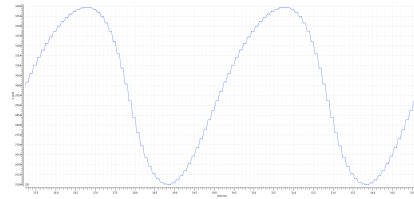


Fig. 14. Switched signal - small L, larger W

IV. CONCLUSION

Ultra low-voltage RtR fully differential switched-capacitor filter with supply voltage of 0.6 V was designed for load capacitance 10 pF. Power consumption of this circuit is 22.16 μW . If necessary, gain of the integrator 24.09 dB can be increased by larger ratio of capacitors $i_{C_{S1}}$ and $i_{C_{S3}}$. It is important to note, that for possibly increase the gain, it is necessary to design output stages of OTA for higher current values.

This switched-capacitor integrator will be used as the main part of currently designing Sigma-Delta analog to digital converter. Mentioned converter will be developed for energy-harvesting applications (solar panels, wind power stations etc.).

ACKNOWLEDGMENT

This work was supported in part by the Ministry of Education, Science, Research and Sport of the Slovak Republic under grant VEGA 1/0731/20, ECSEL JU under project PROGRESSUS (876868) and by the Slovak Research and Development Agency under grant APVV 19-0392.

REFERENCES

- [1] N. Gandhi and S. Shelke, "Sigma delta analog to digital converter: Design and implementation with reduction in power consumption," pp. 1035–1039, 05 2017.
- [2] L. Yao, M. Steyaert, and W. Sansen, *Low-power low-voltage Sigma-Delta modulators in nanometer CMOS*. Springer, 2006.
- [3] Lee, Song, and Roh, "A 103 dB DR Fourth-Order Delta-Sigma Modulator for Sensor Applications," *Electronics*, vol. 8, p. 1093, 09 2019.
- [4] R. Schreier, G. C. Temes, and S. Pavan, *Understanding Delta-Sigma data converters*. Hoboken, New Jersey: John Wiley and sons, Inc., 2nd ed., 2017.
- [5] B. Razavi, *Design of analog CMOS integrated circuit*. McGraw Hill, 1st ed., 2001.